

# Research on the Acoustic Response Characteristics of Stranded Acoustic Sensing Optical Cables

PENG Hao<sup>1</sup>; DU Yong<sup>2</sup>; LUO Zhihui<sup>3,2</sup>; ZENG Shuguang<sup>2</sup>; MAO Peng<sup>1</sup>

1. PowerChina Guiyang Engineering Corporation Limited; 2. College of Mathematics and Physics, China Three Gorges University; 3. Hubei Engineering Research Center of Weak Magnetic-Field Detection, China Three Gorges University

**Abstract:** To address insufficient acoustic sensitivity and significant mid-to-high frequency attenuation in DAS optical cables, a distributed acoustic sensing cable with an externally stranded sensing unit is proposed. Acoustic-field propagation in a four-layer solid-gas composite medium is analyzed, and an acoustic pressure transfer model is established. Finite-element simulation is used to study the effects of sheath Young's modulus and air layer on acoustic response. Stranded and spiral-armored cables based on UW-FBG arrays with 5 m spacing are fabricated, their frequency characteristics are tested, and pipeline leakage monitoring experiments are performed. Results show that the average acoustic pressure sensitivity of the stranded cable is more than 10 dB re 1 rad/ $\mu$ Pa higher than that of the spiral-armored cable, with smaller mid-to-high frequency attenuation. Reducing the Young's modulus of the outer sheath enhances acoustic-field coupling and improves cable acoustic sensitivity, providing guidance for optimized design of acoustic sensing cables.

**Keywords:** distributed acoustic sensing; stranded sensing cable; acoustic pressure sensitivity; ultra-weak fiber Bragg grating array; pipeline leakage

## Figure and Table Captions

Fig. 1 Acoustic-field propagation model of the four-layer medium.

Fig. 2 Relationship between sound-intensity transmission coefficient and E3.

Fig. 3 Simulation models of the stranded and spiral-armored cables.

Fig. 4 Acoustic pressure cloud map and stress distribution of the stranded cable.

Fig. 5 Acoustic pressure cloud map and stress distribution of the spiral-armored cable.

Fig. 6 Relationship between fiber-core stress and sheath modulus and frequency response of the core.

Fig. 7 Test system.

Fig. 8 Frequency response characteristics of the two cables.

Fig. 9 Pipeline leakage field experiment.

Fig. 10 Power spectral density of cable signals.

## 1. Introduction

Distributed acoustic sensing (DAS) has high sensitivity, resistance to high temperature and pressure, corrosion resistance and immunity to electromagnetic interference. It has broad application prospects in pipeline leakage monitoring and acoustic-fingerprint fault diagnosis. As the key sensing unit of a DAS system, the acoustic response characteristics of the sensing cable strongly determine overall system performance, and targeted structural optimization of the cable has become an important direction for improving DAS.

Bare DAS fiber has high sensitivity and fidelity but low strength and poor robustness. Cabling and armored structures significantly improve survival and engineering adaptability in complex environments, but the added mechanical constraints weaken fiber response to external vibration. Prior studies have shown large differences in sensitivity among cable structures, indicating that mechanical design can greatly improve sensor sensitivity and stability.

Helically wound fiber-optic cables can respond sensitively to signals from multiple directions because the fiber is wound helically. However, water and air differ greatly in density and elastic modulus, and their acoustic impedances differ by more than three orders of magnitude. At an air-cable interface, reflection loss is far greater than coupling loss in water. In addition, high-density helical winding introduces optical power loss and involves complex manufacturing, limiting adaptability for long-distance pipeline leak monitoring and belt-conveyor fault monitoring.

This paper proposes a distributed acoustic sensing cable in which the sensing unit adopts an external stranded structure. The acoustic propagation characteristics of a cylindrical multilayer cable are analyzed, a gas-solid-gas/solid-

solid coupled four-layer acoustic-pressure transfer model is established, COMSOL simulation is used to examine key factors affecting acoustic-pressure transfer efficiency, and corresponding DAS cables are fabricated and tested.

## 2. Basic Principles

### 2.1 Acoustic Propagation Theory of Multilayer DAS Cables

The four-layer acoustic-field propagation model of a DAS cable consists of external air, the outer cable sheath, the inner sheath/filling layer and the fiber core. The boundaries between layers are considered ideal acoustic interfaces. A plane harmonic wave generated by an external sound source is assumed to impinge perpendicularly on the cable surface and then pass through the layers to reach the fiber core. Due to characteristic acoustic-impedance mismatch, sound waves are both reflected and transmitted at each interface; this paper focuses on the transmission process toward the fiber.

Each layer is described by density, sound velocity and characteristic acoustic impedance. Solid layers such as the sheath and fiber core are treated as isotropic elastic media in which sound propagates as longitudinal waves. The Young's modulus and density of the cable materials directly determine impedance matching at the interfaces.

Using continuity of sound pressure and particle velocity, the transfer matrix method is used to establish relationships among acoustic fields in the layers. The pressure transmitted into the fiber core is taken as the evaluation indicator for cable acoustic response performance. For a spiral-armored cable, the third layer is air, which acts as an acoustic isolation layer. In a stranded cable, the third layer is a solid inner sheath. Because the modulus of the solid inner layer is far greater than that of air, the inhibitory effect of a high-modulus outer sheath on sound transmission is alleviated, improving the acoustic pressure reaching the fiber.

### 2.2 Simulation Modeling

COMSOL was used to establish three-dimensional acoustic-solid coupled finite-element models of stranded and spiral-armored cables. The stranded cable consists internally of tight-buffered fiber and multiple filling units stranded together to form a compact composite structure, with FRP in the center and good contact among subunits and the outer sheath. The spiral-armored cable contains a sensing fiber loosely located inside the outer sheath, with a relatively thick air layer around it.

Material parameters were assigned based on the actual cable materials, including silica fiber core, FRP and polyethylene sheath. A plane-wave acoustic excitation with an incident pressure amplitude of 0.5 Pa was applied radially to the cable surface. Simulation showed that the equivalent stress amplitude at the fiber core of the stranded cable reached about 18.6 N/m<sup>2</sup>. In contrast, the air layer in the spiral-armored cable caused rapid attenuation of the sound field inside the cable, and the core stress was only about 0.4 N/m<sup>2</sup>.

The results show that cable structure has a decisive influence on acoustic coupling and transfer efficiency, directly limiting the stress response at the fiber core. Under the same external acoustic excitation, a continuous internal solid medium transfers acoustic energy more efficiently.

Simulation of the stranded cable showed that as the Young's modulus of the outer sheath increases, the maximum stress at the fiber core decays exponentially because high modulus causes acoustic-impedance mismatch and reflects incident energy. Increasing the modulus of the inner sheath creates a stiffer acoustic transfer channel, suppresses secondary attenuation inside the cable and helps maintain acoustic coupling efficiency. The natural frequency also shifts from around 1300 Hz to 2400 Hz as sheath modulus increases, indicating that the sensitive frequency band can be designed for specific acoustic monitoring scenarios.

## 3. Cable Fabrication and Testing

### 3.1 Cable Fabrication

Considering the high-frequency response of the cable, a 1.0 mm diameter FRP was selected as the strength member of the stranded cable. A thermoplastic polyurethane (TPU) sensitivity-enhancing layer was extruded around the FRP, increasing its outer diameter to 2.5 mm. Six 0.9 mm filling units were stranded around the FRP center; one unit contained the UW-FBG sensing fiber, and the remaining units provided structural filling and mechanical support. The UW-FBG array had a center wavelength of 1550.12 nm, spectral width greater than 22 nm and grating spacing of 5 μm.

The fiber stranding density was optimized according to intrinsic attenuation to balance acoustic response and transmission performance. An outer thermoplastic elastomer (TPE) protective layer was extruded as the sheath. By introducing TPU and TPE as acoustic coupling media, the structure effectively improves transmission of external sound waves to the fiber core. While meeting tensile and engineering installation requirements, the cable can be directly attached to pipes, belt conveyors and other equipment.

## 3.2 Acoustic Characteristics Test

To verify the acoustic response differences of cable structures, the frequency-response characteristics of the stranded and spiral-armored cables were compared. The test system included a DAS demodulation module, host computer, dedicated speaker and sound-level meter. Each cable was about 25 m long and was coiled inside a sound-absorbing box to reduce environmental echo and reflection. A computer-controlled audio generator output constant-amplitude sinusoidal sweep signals, which impinged perpendicularly on the cable surface. The DAS system demodulated and recorded fiber phase response, while the sound-level meter recorded incident sound pressure at the cable position.

The stranded cable showed higher acoustic pressure sensitivity throughout the test band, with slower attenuation at high frequencies and clear resonance enhancement at several frequencies. Sensitivity was about -112 dB re 1 rad/ $\mu$ Pa at 1200 Hz, about -120 dB re 1 rad/ $\mu$ Pa at 2400 Hz and again about -112 dB re 1 rad/ $\mu$ Pa near 4000 Hz. The spiral-armored cable, because its third layer is air, showed slightly higher response only at a few resonance points and was generally at least 10 dB re 1 rad/ $\mu$ Pa lower in other frequency ranges, with rapid attenuation above 2000 Hz.

## 3.3 Pipeline Leakage Monitoring Experiment

An outdoor test system was built to further evaluate the practical performance of the two cables in gas-pipeline leakage monitoring. The stranded and spiral-armored cables were fixed about 1 m from the gas pipe, and a leakage valve was adjusted to simulate the leak source. To eliminate instrument differences, the two cables were fusion-spliced in series and connected to the same DAS demodulator.

Welch power spectral density estimation was used to analyze the acquired time-domain signals and improve spectral stability. Under the same leakage-source excitation, the PSD of the stranded cable was generally higher than that of the spiral-armored cable in the main leakage-frequency band, demonstrating stronger acoustic response and higher sensitivity. The results confirm that cable structure strongly affects the coupling path from external sound source to cable structure and finally to the fiber core.

## 4. Conclusion

This paper proposes and verifies a UW-FBG DAS cable based on a stranded structure and applies it to pipeline leakage sound-field monitoring. A four-layer cylindrical acoustic-transfer model was established. Simulation shows that the acoustic sensitivity of the stranded cable is generally better than that of a spiral-armored cable and attenuates more slowly as frequency increases. Reducing the Young's modulus of the outer sheath can significantly improve acoustic monitoring sensitivity.

Stranded and spiral-armored cables were fabricated and tested. Experimental results verified that the stranded cable improves sensitivity by about 10 dB re 1 rad/ $\mu$ Pa compared with the spiral-armored cable. The stranded cable balances high sensitivity and engineering economy, and its acoustic coupling advantage in air makes it suitable for pipeline leakage and other acoustic monitoring applications.

## References

*Reference entries are retained in the original citation form to avoid altering source bibliographic data.*

- [1] 邹辉,谢欣. 分布式光纤声波传感及其进展研究[J/OL]. 光通信研究,1-14[2024-12-21]. <http://kns.cnki.net/kcms/de-tail/42.1266.TN.20240724.1602.004.html>.
- [2] 孙琪真,李豪,范存政,等.基于散射增强光纤的分布式声波传感研究进展[J].激光与光电子学进展,2022,59(21):9-26.
- [3] 范存政,石正宣,陶禹然,等.椭圆缠绕式分布式光纤矢量声波传感器技术研究(特邀)[J].红外与激光工程,2025,54(04):279-288.
- [4] HAN B, GUAN H, YAO J, et al. Distributed Acoustic Sensing With Sensitivity-Enhanced Optical Cable[J/OL]. IEEE Sensors Journal, 2021, 21(4): 4644-4651. DOI:10.1109/JSEN.2020.3035002.
- [5] SHANG Y, WANG C, NI J sheng, et al. Discussion on the sensitivity of optical cables based on distributed acoustic sensing[J]. Optical Review, 2019, 26(6): 659-663.
- [6] 陆祈祯,黄俊斌,顾宏灿,等.一种耐静压分布反馈式光纤激光水听器探头设计[J].应用光学,2020,41(02):428-434.
- [7] 林融冰,包丰,谢军,等.光缆布设方式对 DAS 主、被动源记录的影响[J].地球物理学报,2022,65(10):4087-4098.
- [8] 邓宝,李俊伦,方大为,等.不同类型光缆对地表和井中分布式声波传感信号质量的影响研究[J].地震学报,2025,47(04):569-593.

- [9] INNANEN K A, LAWTON D, HALL K, et al. Design and deployment of a prototype multicomponent distributed acoustic sensing loop array[C]//SEG Technical Program Expanded Abstracts 2019. San Antonio, Texas: Society of Exploration Geophysicists, 2019: 953-957.
- [10] KUVSHINOV B N. Interaction of helically wound fibre-optic cables with plane seismic waves[J]. Geophysical Prospecting, 2016, 64(3): 671-688.
- [11] 曹丹平,律军军,孙上饶,等.基于螺旋缠绕光纤的分布式声波传感三分量信号采集机理研究[J].石油物探,2022,61(01):60-69.
- [12] 聂俊光,徐德宝,姚宇晖,等.分布式螺旋光缆 DAS 地震采集系统与地震检波器对比试验[J/OL].地球物理学进展,2026,1-18.
- [13] 杜功焕,朱哲民,龚秀芬.声学基础[M].南京:南京大学出版社:2001:183.
- [14] 张嘉伟,胡昊灏,黄一帆,等.基于传递矩阵法的声学覆盖层透射系数预报研究[J].噪声与振动控制,2024,44(01):80-85.

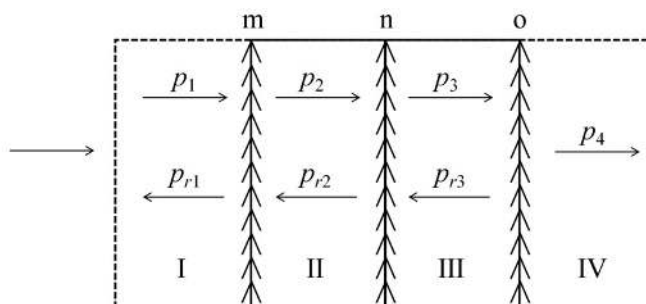
作者简介: 彭浩 (1988—), 正高级工程师, 硕士, 主要从事岩土工程安全监测。E-mail: penghaoslamdunk@yeah.net

通信作者: 志 (1975—), 副教授, 博士, 主要从事光纤传感技术及其应用研究。E-mail: zhihui\_luo@126.com

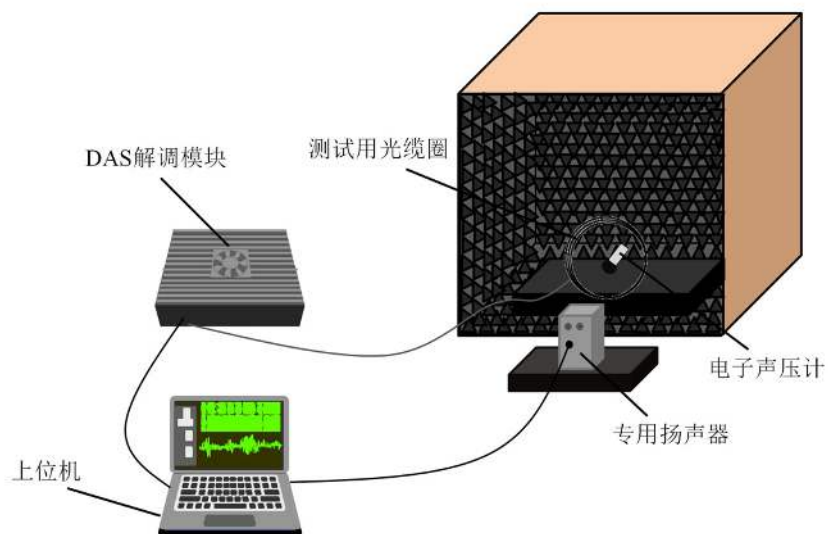
## Retained Figures and Visual Materials

The original figures, screenshots, diagrams and experimental plots from the source manuscript are retained below in their original order for layout continuity. Captions in the translated body follow the source numbering where available.

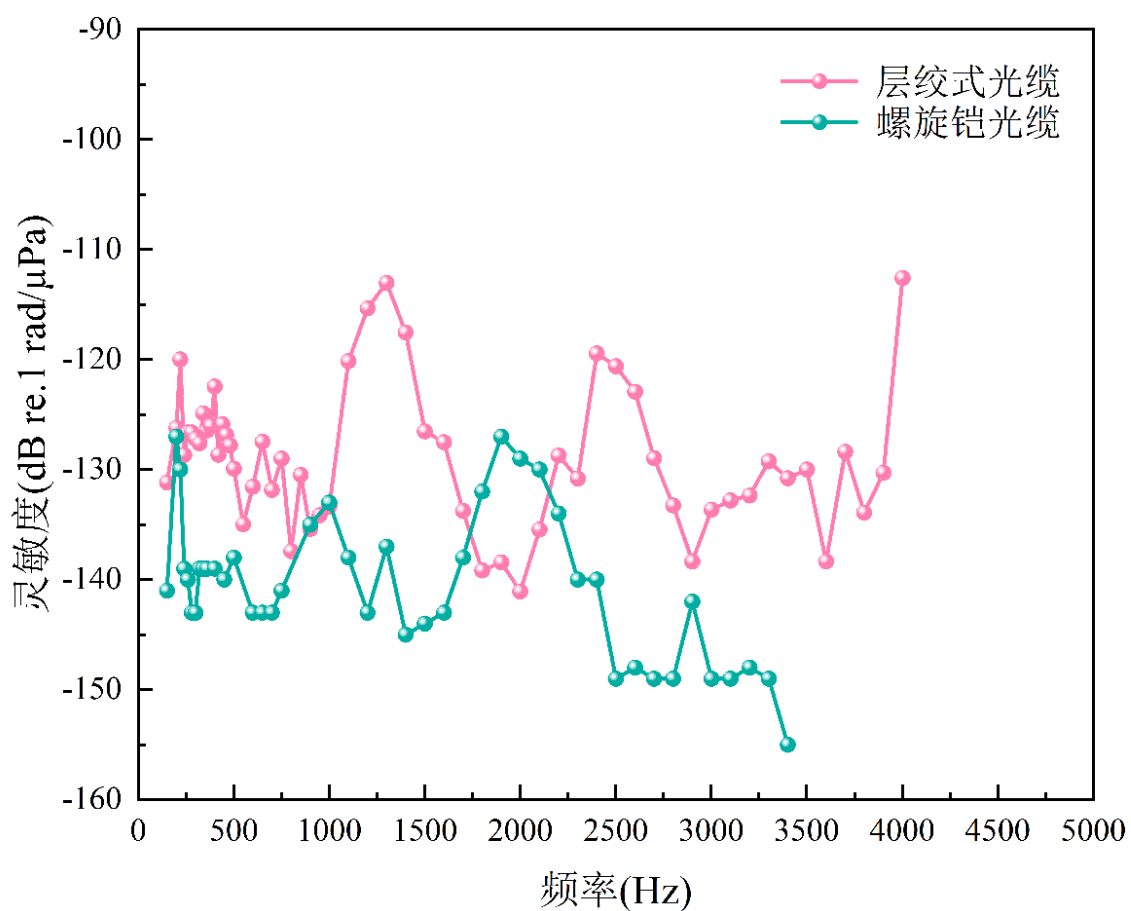
### Original visual material 1



### Original visual material 2



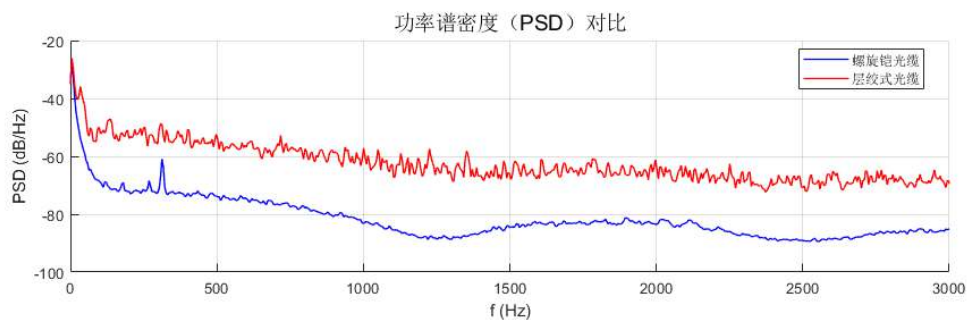
Original visual material 3



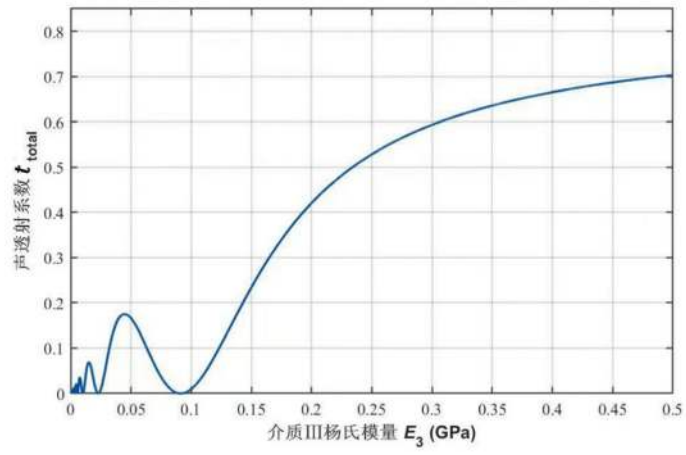
Original visual material 4



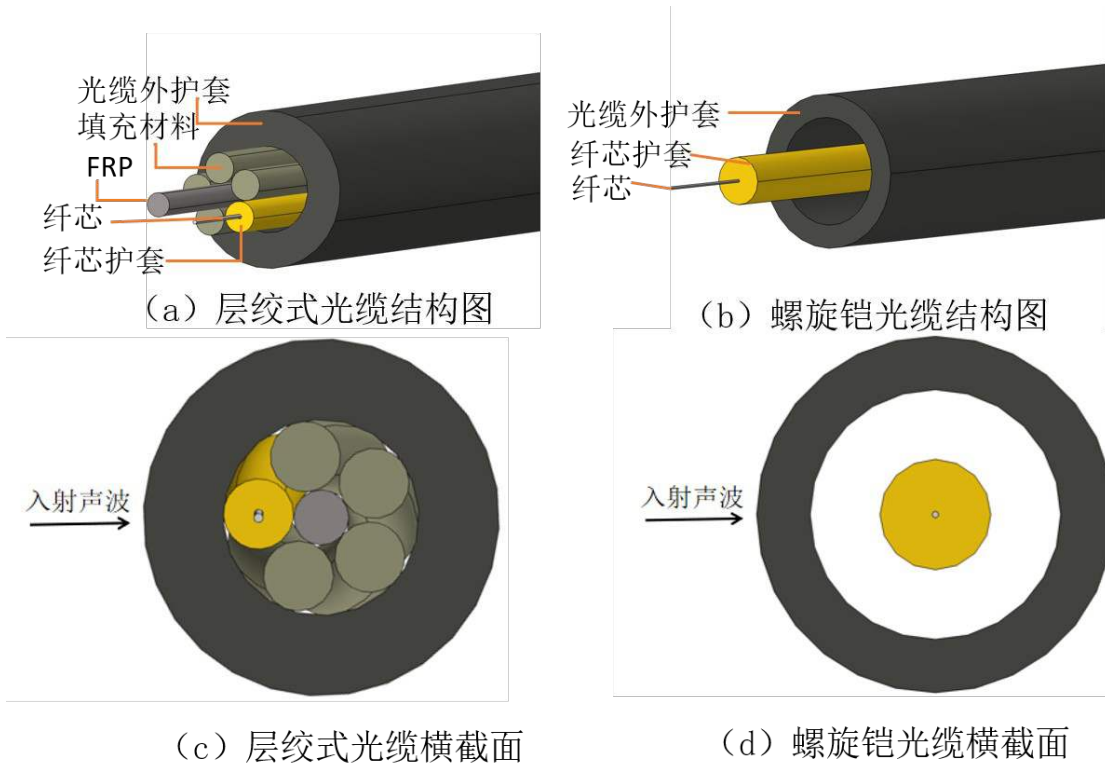
Original visual material 5



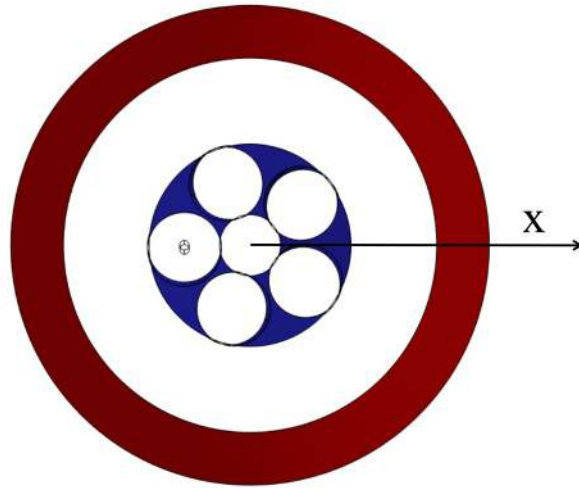
Original visual material 6



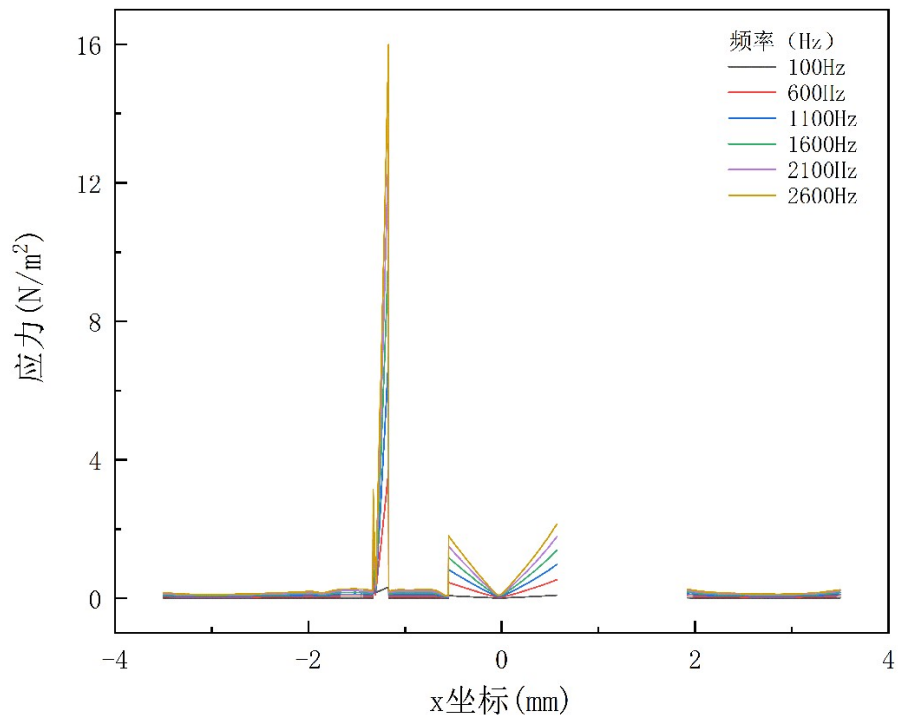
Original visual material 7



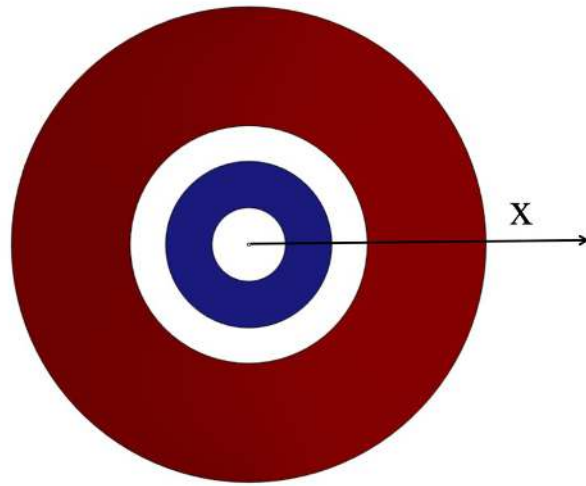
Original visual material 8



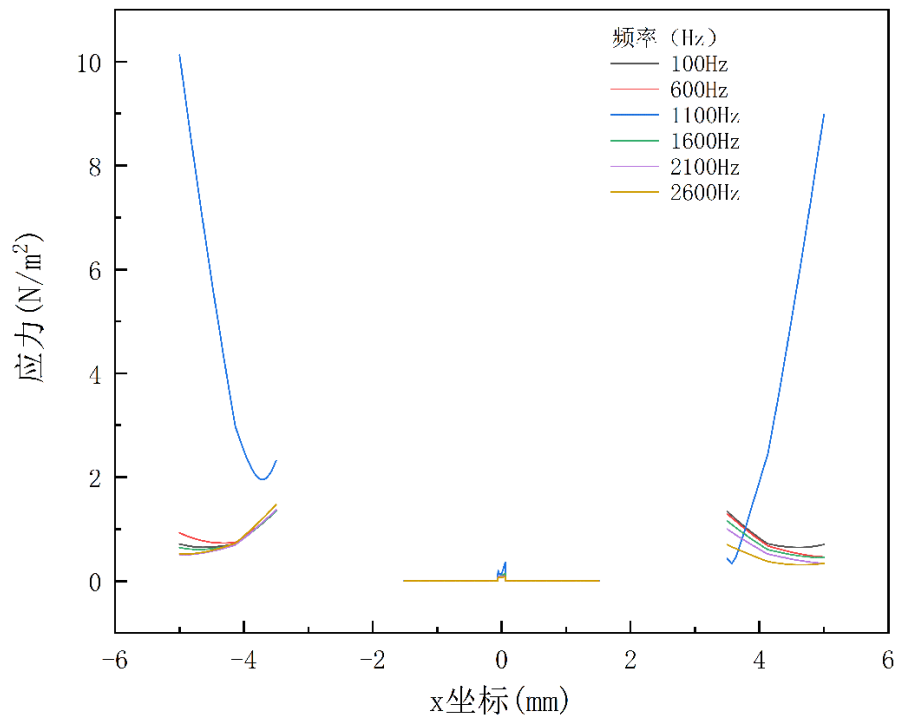
Original visual material 9



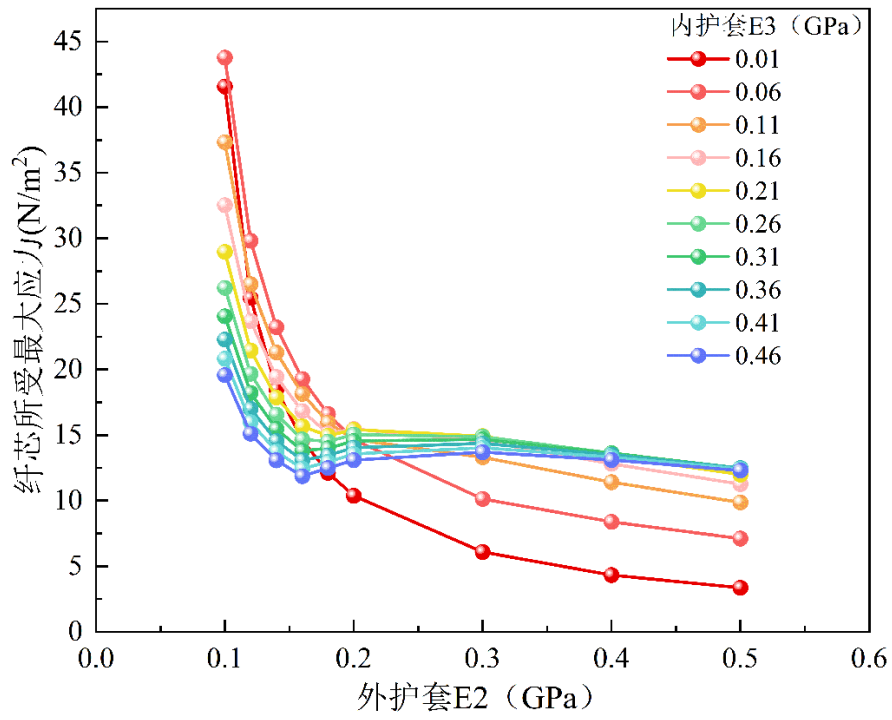
Original visual material 10



Original visual material 11



Original visual material 12



Original visual material 13

